``Enseigner la recherche en train de se faire''

COLLÈGE DE FRANCE 1530

Chaire de
Physique de la Matière Condensée

PETITS SYSTEMES THERMOELECTRIQUES: *CONDUCTEURS MESOSCOPIQUES ET GAZ D'ATOMES FROIDS*

Cycle « Thermoélectricité »
2012 - 2014

Antoine Georges

Séance du 19 novembre 2013
Cours 4

Thermal Transport in the Quantum Regime.
Connections to Information Theory.

Séminaire :
Olivier Bourgeois (Institut Néel, Grenoble)

Nanophononique : du transport de phonons à basse température aux applications en thermoélectricité

The Wiedemann-Franz Law and the Quantum of Thermal Conductance

Thermal conductance of a perfectly ballistic single channel as T→ 0:

$$\boxed{\frac{G_{th}}{T} \rightarrow \frac{\pi^2}{3}\frac{k_B^2}{h}}$$

per spin component

(= 9.456 10^{-13} W/K^2 ~ 1pW/K^2)

Compare electrical conductance, again per spin channel:

$$G \rightarrow \frac{e^2}{h}$$

Wiedemann-Franz law, Lorenz number:

$$\frac{G_{th}/T}{G} \equiv \mathcal{L} \rightarrow \left(\frac{k_B}{e}\right)^2 \frac{\pi^2}{3}$$

Recall derivation: $I_n \equiv \int d\varepsilon\, \mathcal{T}(\varepsilon) \left(\frac{\varepsilon-\mu}{k_B T}\right)^n \left(-\frac{\partial f}{\partial \varepsilon}\right)$

$$G = \frac{2e^2}{h} I_0$$

$$\frac{G_{th}}{T} = \frac{2}{h} k_B^2 \left[I_2 - \frac{I_1^2}{I_0}\right]$$

$$\mathcal{L} \equiv \frac{G_{th}}{TG} = \left(\frac{k_B}{e}\right)^2 \left[\frac{I_2}{I_0} - \left(\frac{I_1}{I_0}\right)^2\right]$$

Sommerfeld's expansion as $T \rightarrow 0$:

$$f(\varepsilon-\mu) = \theta(\mu-\varepsilon) - \frac{\pi^2}{6}(k_B T)^2\, \delta'(\varepsilon-\mu) + \cdots$$

The terms involving I_1 drop out as $T \rightarrow 0$
In I_2, the derivatives of the transmission coefficient don't contribute as $T \rightarrow 0$

What about bosons ?
(phonons, photons,…)

cf: Maynard and Akkermans, PRB 32, 5440 (1985)
Greiner et al. PRL 78, 1114 (1997)
Rego and Kirczenow, PRL 81, 232 (1998)

1 bosonic mode, non-conserved number (μ=0) e.g phonon, photon :

A. Non-conserved bosons

Non-conserved bosons $\mu_L = \mu_R = 0$, but thermal gradient $T_L - T_R \equiv \Delta T$. Consider a single mode. Energy current:

$$I_E = \int_{k>0} \frac{dk}{2\pi} v_k \, \hbar\omega_k \, [b_L - b_R] \, \mathcal{T}(\omega_k) \ , \tag{41}$$

with $b_{L,R}$ the Bose distribution of each reservoir:

$$b(\omega) \equiv \left[\exp \frac{\hbar\omega}{k_B T} - 1\right]^{-1} \ , \ \frac{\partial b}{\partial T} = \frac{1}{T} \frac{\hbar\omega}{k_B T} g\left(\frac{\hbar\omega}{k_B T}\right) \ , \ g(x) \equiv \frac{1}{4\sinh^2(x/2)} \tag{42}$$

And the group velocity, which cancels with the density of states as usual:

$$v_k = \frac{\partial\omega_k}{\partial k} \ \Rightarrow \int_{k>0} \frac{dk}{2\pi} v_k \, F(\omega_k) = \int \frac{d\omega}{2\pi} F(\omega) \tag{43}$$

In the linear response regime, we thus obtain the expression of the thermal conductance, changing variables to $x \equiv \hbar\omega/k_B T$:

$$G_{\rm th} \equiv \frac{1}{\Delta T} I_E = \frac{k_B^2}{h} T \int_{x_m}^{\infty} dx\, x^2 g(x)\, \mathcal{T}\left(x \frac{k_B T}{\hbar}\right) \tag{44}$$

We have used that $\mu = 0$, so that the energy current also coincides with the heat current ($dE = TdS + \mu dN = TdS = \delta Q$). Here, $x_m = \hbar\omega_{min}/k_B T$ corresponds to the minimal frequency of the mode. In the $T \to 0$ limit, only the gapless modes with $x_m = 0$ contribute to dominant order, e.g. acoustic phonon modes or long-wavelength photon modes. One thus obtains:

$$\boxed{\frac{G_{\rm th}}{T} \to \frac{\pi^2}{3} \frac{k_B^2}{h} \mathcal{T}(0) \le \frac{\pi^2}{3} \frac{k_B^2}{h}} \tag{45}$$

where we have used $\int_0^\infty dx\, x^2 g(x) = \pi^2/3$.

The same universal value applies to bosons and fermions !

Generalization to Quasiparticles with Fractional Statistics

[in the sense of Haldane PRL 67, 937 (1991); Wu PRL 73, 922 (1994)]

Rego and Kircenow, PRB 59, 13080 (1999); Krive and Mucciolo PRB 60, 1429 (1999)

Haldane's exclusion statistics:

$$f_g(x) = \frac{1}{g + W_g(x)} \quad , \quad W^g[1+W]^{1-g} = e^x \quad , \quad x \equiv \frac{\varepsilon - \mu}{k_B T}$$

$$\left(-\frac{\partial f_g}{\partial x}\right) dx = -df_g = \frac{dW}{(W+g)^2}$$

Perfect ballistic single channel:

$$I_n = \int dx\, x^n \left(-\frac{\partial f_g}{\partial x}\right)$$

$$= \int_0^\infty dW \, \frac{[g \ln W + (1-g)\ln(1+W)]^n}{(W+g)^2}$$

$$\Rightarrow I_0 = \frac{1}{g} \quad , \quad I_1 = 0 \quad , \quad \boxed{I_2 = \frac{\pi^2}{3}}$$

I_2 is independent of g (of statistics) !

Hence, universal thermal conductance <u>independent of statistics</u> for a single ballistic channel !

Quasiparticles of charge q obeying g-statistics:

$$G = \frac{q^2}{h}\frac{1}{g} \ ,$$

$$\frac{G_{th}}{T} = \frac{k_B^2}{h}\frac{\pi^2}{3} \ ,$$

$$\mathcal{L} = \left(\frac{k_B}{q}\right)^2 \frac{\pi^2}{3} g$$

Deeper meaning:

Quantum limits
to the flow
of information
and entropy

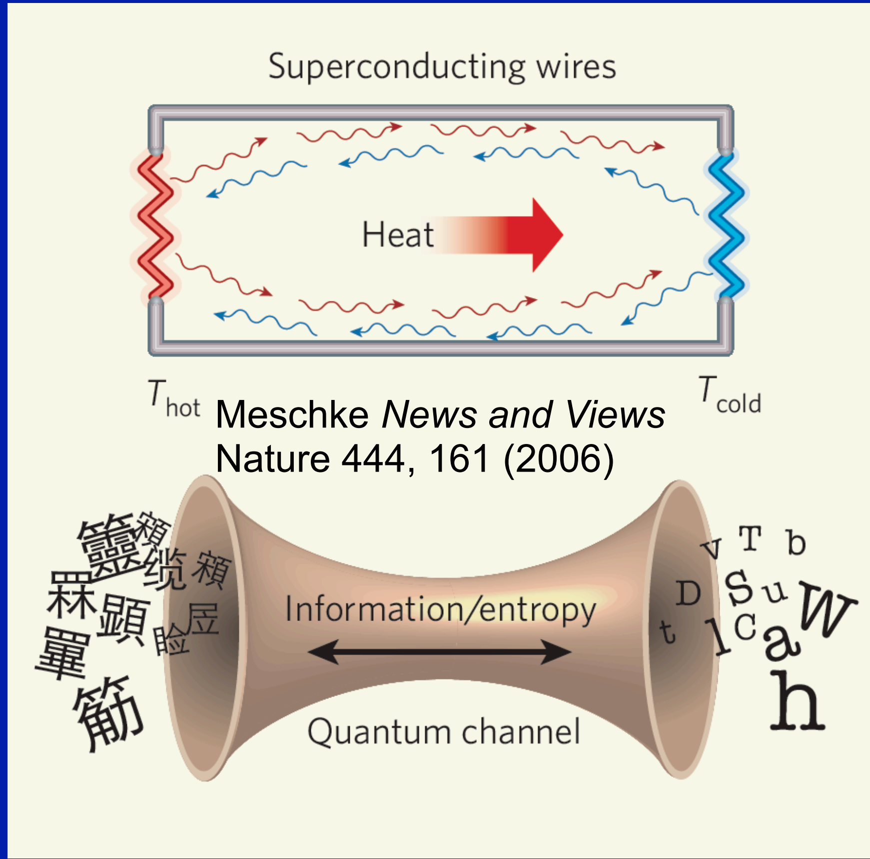

- References:
  - Lebedev and Levitin, Information and Control 9, 1 (1966)
  - Pendry, J.Phys A: Math. Gen. 16, 2161 (1983)
  - Caves and Drummond Rev Mod Phys 66, 481 (1994)
  - Blencowe and Vitelli, Phys Rev A 62, 052104 (2000)
  - Akkermans, Eur. Phys. J. E 28, 1999 (2009)

Pendry's argument and bound

J.B. Pendry J.Phys A 16, 2161 (1983)

- N bits of information transmitted in time t
- Entropy (information) flow: $I_S \sim k_B\, N/t \;\; (\mathcal{C}_{in} \sim \dfrac{N}{t \ln 2})$
- Detection: arrival/non-arrival of a particle
- Energy cannot be resolved better than $\delta E \simeq \hbar/t$
- Energies spread over $N\delta E \simeq N\hbar/t$
- Mean energy per particle: $\dfrac{t}{N\hbar}\displaystyle\int_0^{N\hbar/t} d\epsilon\, \epsilon \sim \frac{1}{2}\frac{N\hbar}{t}$
- Energy current (= power of signal P) is at least:

$$I_E \geq \hbar N^2 t^{-2}/2$$

Hence:

(with c a numerical constant)

$$\boxed{I_S^2 \;\leq\; c\,\frac{k_B^2}{h}\,I_E \;,\;\; \left(\mathcal{C} \leq \frac{\sqrt{c}}{\ln 2}\sqrt{\frac{\mathcal{P}}{h}}\right)} \qquad c = \frac{2\pi^2}{3}$$

The Mathematical Problem:

A single (spinless) ballistic channel

$$I_N^\alpha = \frac{1}{h}\int d\varepsilon\, f_g^\alpha \ , \ I_E^\alpha = \frac{1}{h}\int d\varepsilon\, \varepsilon\, f_g^\alpha \ , \ I_S^\alpha = \frac{k_B}{h}\int d\varepsilon\, F_g\left[f_g^\alpha\right]$$

$$I \equiv I^L - I^R$$

$$\alpha = L, R; \ \ f_g^\alpha = f_g\left(\frac{\varepsilon - \mu_\alpha}{k_B T_\alpha}\right)$$

$$g = 1: \ \ f_1(x) = \frac{1}{1+e^x} \ , \ F_1[f] = -f\ln f - (1-f)\ln(1-f)$$

$$\boxed{I_S^2 \leq \frac{2\pi^2}{3}\frac{k_B^2}{h} I_E} \ , (T_L > T_R, \mu_L \geq \mu_R)$$

General proof: ??

Note that this bound by itself does not yield a bound on thermal conductivity

cf.Blencowe and Vitelli PRA 62, 052104 (2000)

see however Akkermans EPJE, 2009

Constrains the heat dissipated to a T=0 outside reservoir by a `black body' at temperature T ($\mu_L=\mu_R=0$; $T_R=0$) :

$$\dot{Q} \leq \frac{2\pi^2}{3}\frac{k_B^2}{h}T^2$$

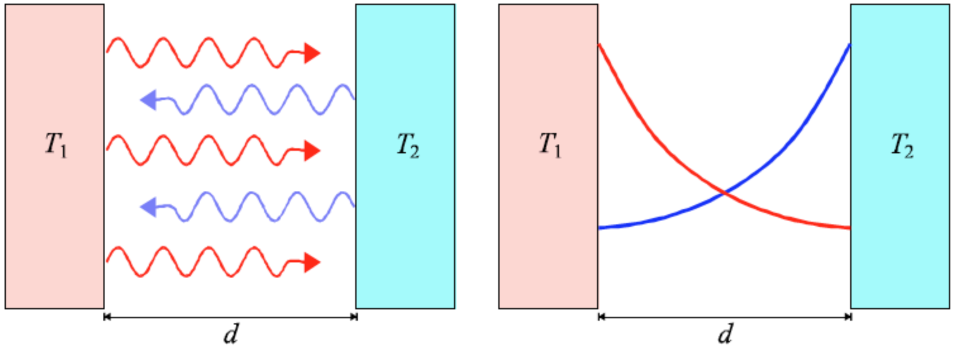

Figure 1. There are two modes for exchange of heat between two surfaces separated by vacuum: conventional radiative transfer, or photon tunnelling via evanescent states. The latter dominate at short distances. See table 1.

JB Pendry J.Phys. Cond Mat 11, 6621 (1999)

Blencowe and Vitelli suggest a tighter bound for fermions which does yield the expected limit on the thermal conductance:

$$I_S^2 \leq \frac{2\pi^2}{3}\frac{k_B^2}{h}\frac{T_L-T_R}{T_L+T_R}(I_E-\mu I_N)$$

$$(\mu_L=\mu_R=\mu, T_L>T_R)$$

EXPERIMENTS

- Phonons
- Photons
- Electrons

PHONONS

THEORY -
From Rego and Kircenow PRL 81, 232 (1998)

$$\kappa = \frac{k_B^2 \pi^2}{3h} T N_\alpha + \frac{k_B^2}{h} T \sum_{\alpha'}^{N_{\alpha'}} \left\{ \frac{\pi^2}{3} + f(x_0) + \frac{x_0^2 e^{x_0}}{e^{x_0} - 1} \right\},$$

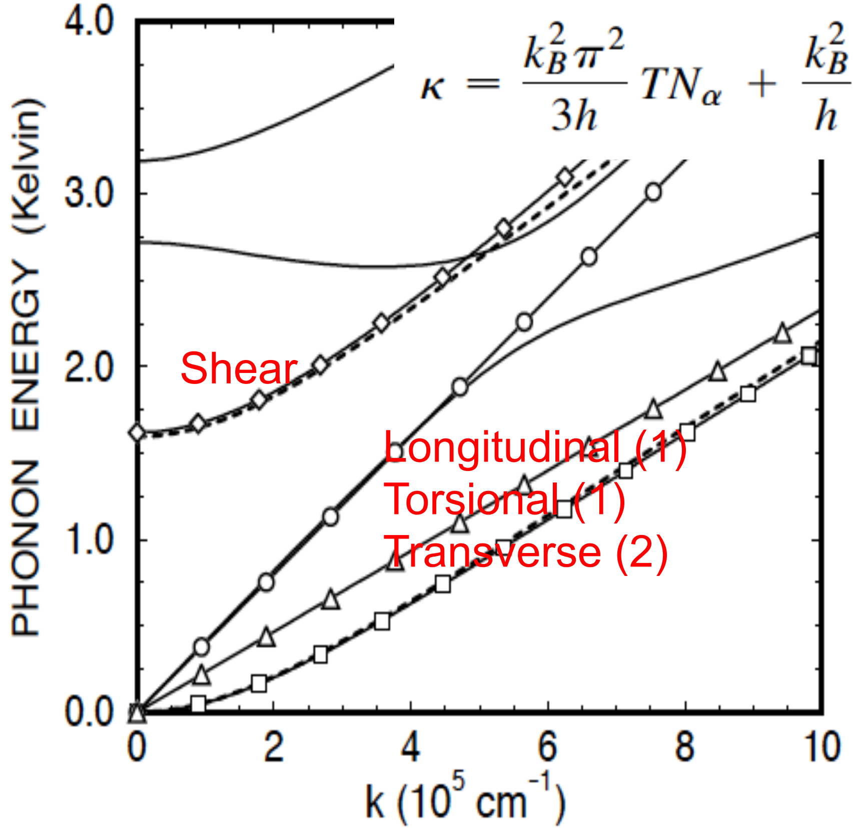

FIG. 1. Lowest energy acoustic modes of a quasi-2D system of thickness 50 nm and of a long wire of square cross section 50 nm × 50 nm. Thick solid (dashed) lines represent the symmetric (antisymmetric) modes of the quasi-2D system. Thin lines with circles, squares, diamonds, and triangles represent the longitudinal, transverse, shear, and torsional modes of the wire, respectively. The elastic parameters are for GaAs.

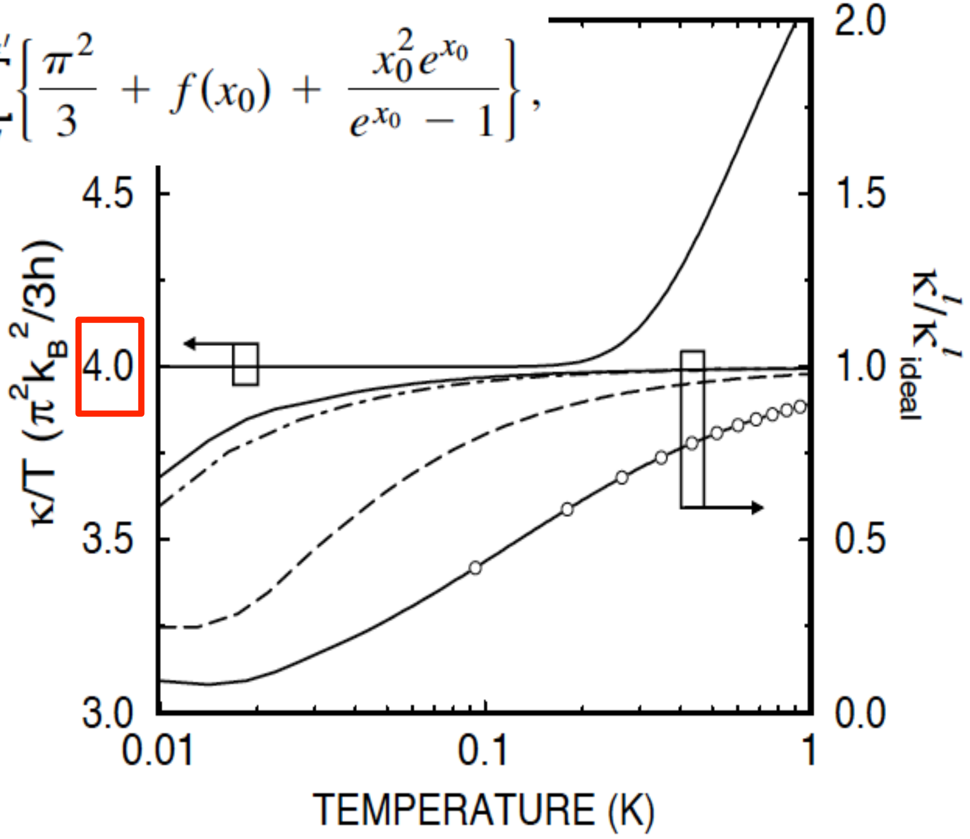

FIG. 3. Left scale: Thermal conductance of a quantum wire with ideal contacts divided by temperature. Right scale: Contribution to thermal conductance due to the longitudinal mode for various contact shapes; *infinite catenoid* for $\lambda = 4.6\mu$ (solid line), finite catenoid for $\lambda = 4.6\mu$ (dot-dashed line), catenoid with $\lambda = 0.86\mu$ (long-dashed line), and conic for $\theta = \pi/6$ (solid line with circles). $\kappa_{\rm ideal}^{l} = k_B^2 \pi^2 T/3h$.

Measurement of the quantum of thermal conductance

K. Schwab*, E. A. Henriksen*, J. M. Worlock*† & M. L. Roukes*

** Condensed Matter Physics 114-36, California Institute of Technology, Pasadena, California 91125, USA*

Schwab et al. Nature 404,974 (2000)

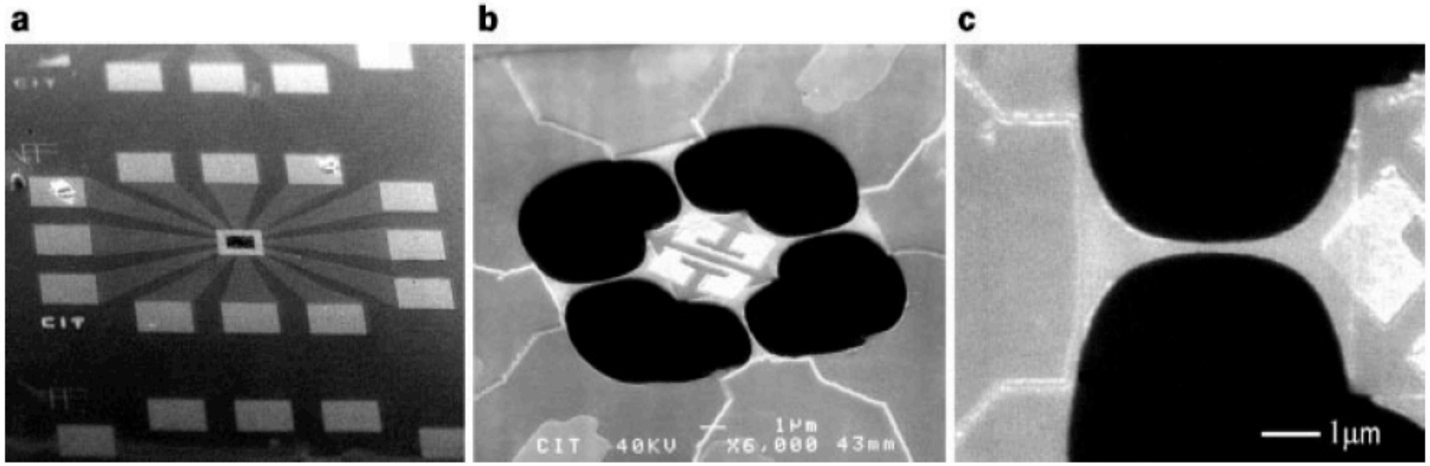

Figure 1 Suspended mesoscopic device. A series of progressive magnifications are shown. **a**, Overall view of the ~1.0 × 0.8 mm device, showing 12 wirebond pads that converge via thin-film niobium leads into the centre of the device. This central region is a 60-nm-thick silicon nitride membrane, which appears dark in the electron micrograph. **b**, View of the suspended device, which consists of a 4 × 4 μm 'phonon cavity' (centre) patterned from the membrane. In this view, the bright "c" shaped objects on the device are thin-film gold transducers, whereas in the dark regions the membrane has been completely removed. The transducers are connected to thin-film. niobium leads that run atop the 'phonon waveguides'; these leads ultimately terminate at the wirebond pads. **c**, Close-up of one of the catenoidal waveguides, displaying the narrowest region which necks down to <200-nm width.

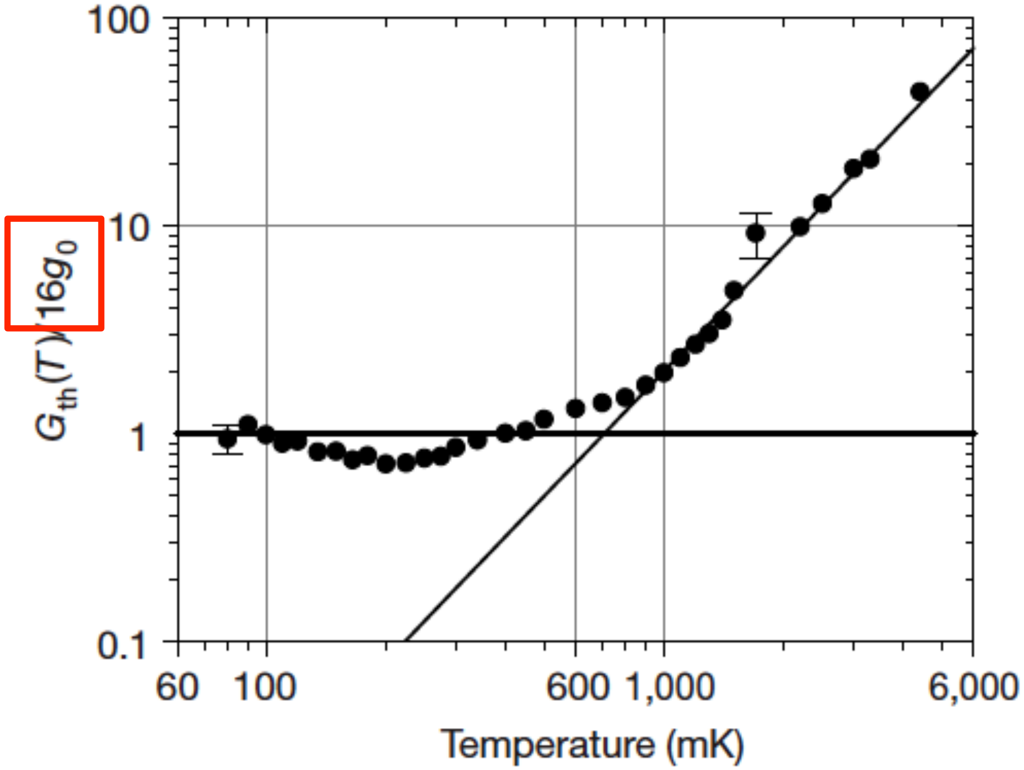

Figure 3 Thermal conductance data. We normalize the measured thermal conductance by the expected low-temperature value for 16 occupied modes, 16 g_0. Measurement error is approximately the size of the data points, except where indicated. For temperatures above $T_{co} \approx 0.8$ K, we observe a cubic power-law behaviour consistent with a mean free path of $\sim$0.9 μm. For temperatures below T_{co}, we observe a saturation in G_{th} at a value near the expected quantum of thermal conductance. Consistent with expectations, to within experimental uncertainty, G_{th} never exceeds 16 g_0 once it finally drops below that value. The (implicit) linear temperature dependence observed for $T < T_{co}$ is the hallmark of one-dimensional thermal transport. The approximate saturation at the maximum expected magnitude, $G_{th} \approx 16$ g_0, indicates that both the ballistic and adiabatic conditions have been satisfied in these experiments.

PHOTONS

Vol 444 | 9 November 2006 | doi:10.1038/nature05276

Nature 444, 187 (2006)

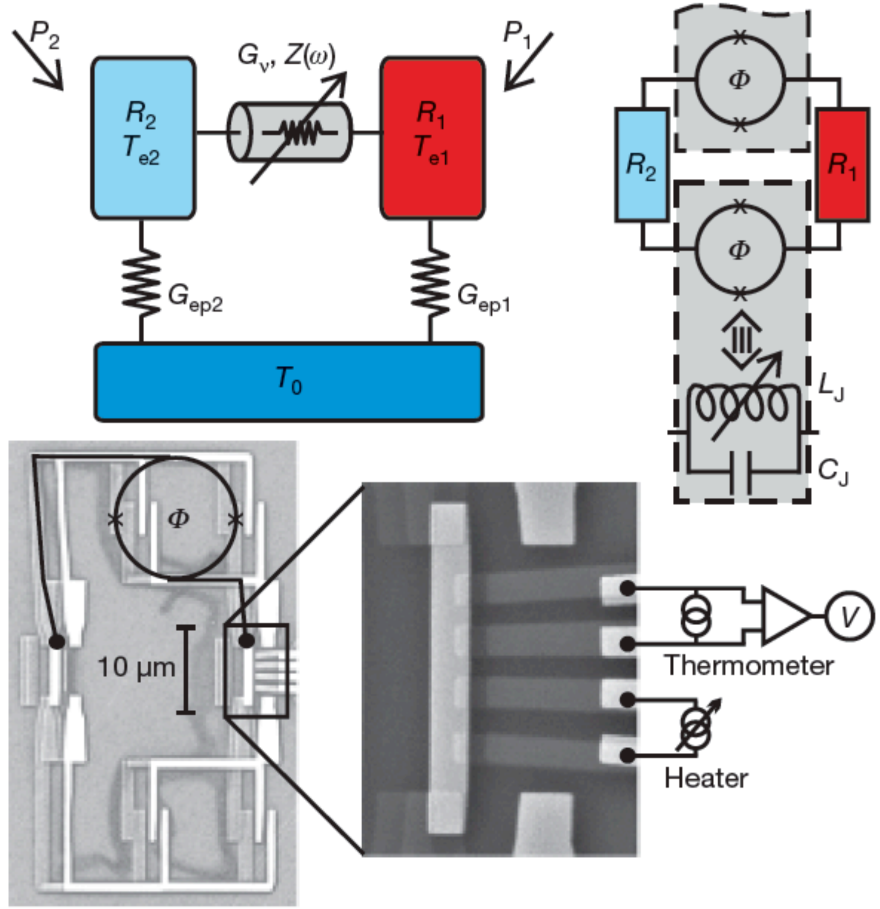

Figure 1 | The system under investigation. At the top, we show thermal (left) and electrical (right) models; at the bottom, a scanning electron micrograph of the device (left), and a magnified view of resistor 1 with four adjoining NIS and two NS contacts (right). See text for details.

Single-mode heat conduction by photons

Matthias Meschke[1], Wiebke Guichard[1,2] & Jukka P. Pekola[1]

ELECTRONS

Quantum Limit of Heat Flow Across a Single Electronic Channel

S. Jezouin,[1*] F. D. Parmentier,[1*] A. Anthore,[1,2†] U. Gennser,[1] A. Cavanna,[1] Y. Jin,[1] F. Pierre[1†]

http://www.lpn.cnrs.fr/fr/Commun/Actualites/2013-10-29-Pierre-Courant_chaleur.php

Quantum physics predicts that there is a fundamental maximum heat conductance across a single transport channel and that this thermal conductance quantum, G_Q, is universal, independent of the type of particles carrying the heat. Such universality, combined with the relationship between heat and information, signals a general limit on information transfer. We report on the quantitative measurement of the quantum-limited heat flow for Fermi particles across a single electronic channel, using noise thermometry. The demonstrated agreement with the predicted G_Q establishes experimentally this basic building block of quantum thermal transport. The achieved accuracy of below 10% opens access to many experiments involving the quantum manipulation of heat.

[1]CNRS, Laboratoire de Photonique et de Nanostructures, UPR20, route de Nozay, 91460 Marcoussis, France. [2]Univ Paris Diderot, Sorbonne Paris Cité, Département de Physique, 4 rue Elsa Morante, 75013 Paris, France

*These authors contributed equally to this work.
†Corresponding author. E-mail: anne.anthore@lpn.cnrs.fr (A.A.); frederic.pierre@lpn.cnrs.fr (F.P.)

602 1 NOVEMBER 2013 VOL 342 SCIENCE

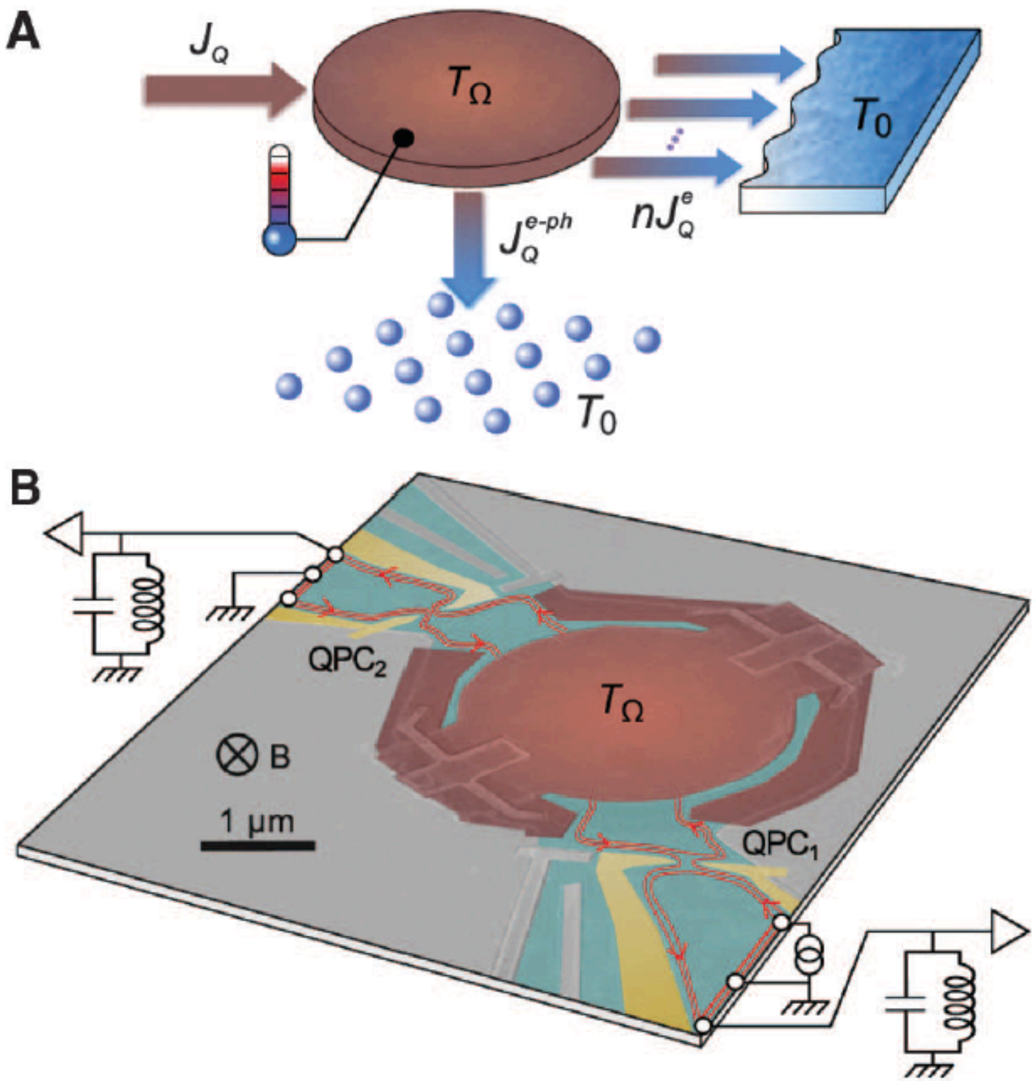

Fig. 1. Experimental principle and practical implementation. (**A**) Principle of the experiment: Electrons in a small metal plate (brown disk) are heated up to T_Ω by the injected Joule power J_Q. The large arrows symbolize injected power (J_Q) and outgoing heat flows (nJ_Q^e, $J_Q^{e\text{-}ph}$). (**B**) False-colors scanning electron micrograph of the measured sample. The Ga(Al)As 2D electron gas is highlighted in light blue, the QPC metal gates in yellow and the micrometer-sized metallic ohmic contact in brown. The light gray metal gates are polarized with a strong negative gate voltage and are not used in the experiment. The propagation direction of two co-propagating edge channels (shown out of $\nu = 3$ or $\nu = 4$) is indicated by red arrows. QPC$_1$ is here set to fully transmit a single channel ($n_1 = 1$) and QPC$_2$ two channels ($n_2 = 2$), corresponding to a total number of open electronic channels $n = n_1 + n_2 = 3$. The experimental apparatus is shown as a simplified diagram. It includes two $L - C$ tanks used to perform the noise thermometry measurements around 700 kHz. The Joule power J_Q is injected on the micrometer-sized metallic electrode from the DC polarization current partly transmitted through QPC$_1$.

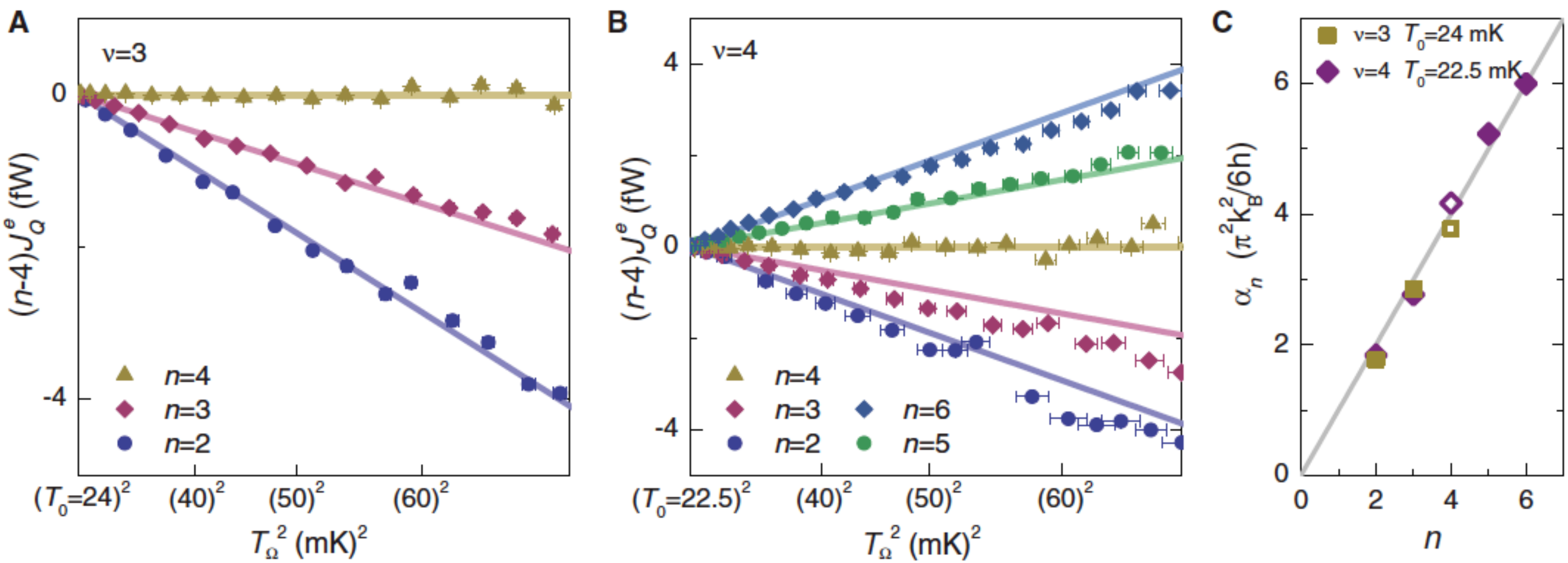

Fig. 3. Heat flow across ballistic electronic channels. (**A** and **B**) The symbols display the heat current across $|n-4|$ electronic channels, with a positive (negative) sign for $n > 4$ ($n < 4$), as a function of the squared temperature T_Ω^2 of the micrometer-sized ohmic contact. The data in (A) [(B)] were measured at $\nu = 3$ ($\nu = 4$) at a base temperature $T_0 = 24$ mK ($T_0 = 22.5$ mK) for n = 2, 3, and 4 (n = 2, 3, 4, 5, 6), respectively from bottom to top. The continuous lines are the theoretical predictions for the quantum-limited heat flow. (**C**) Extracted electronic heat current factor $\alpha_n \equiv nJ_Q^e/(T_\Omega^2 - T_0^2)$ in units of $\pi^2k_B^2/6h$ (symbols) versus the number n of electronic channels. It is obtained from the fitted slopes α'_{n-4} of the data in (A) and (B) added to the separately extracted value of α_4 (see text and Fig. 2): $\alpha_n = \alpha'_{n-4} + \alpha_4$, with $\alpha_4 = 3.8$ ($\alpha_4 = 4.2$) at $\nu = 3$ ($\nu = 4$) shown distinctly as open symbols. The predictions for the quantum limit of heat flow fall on the continuous line $y = x$.

Manipulating thermal currents with magnetic fields !

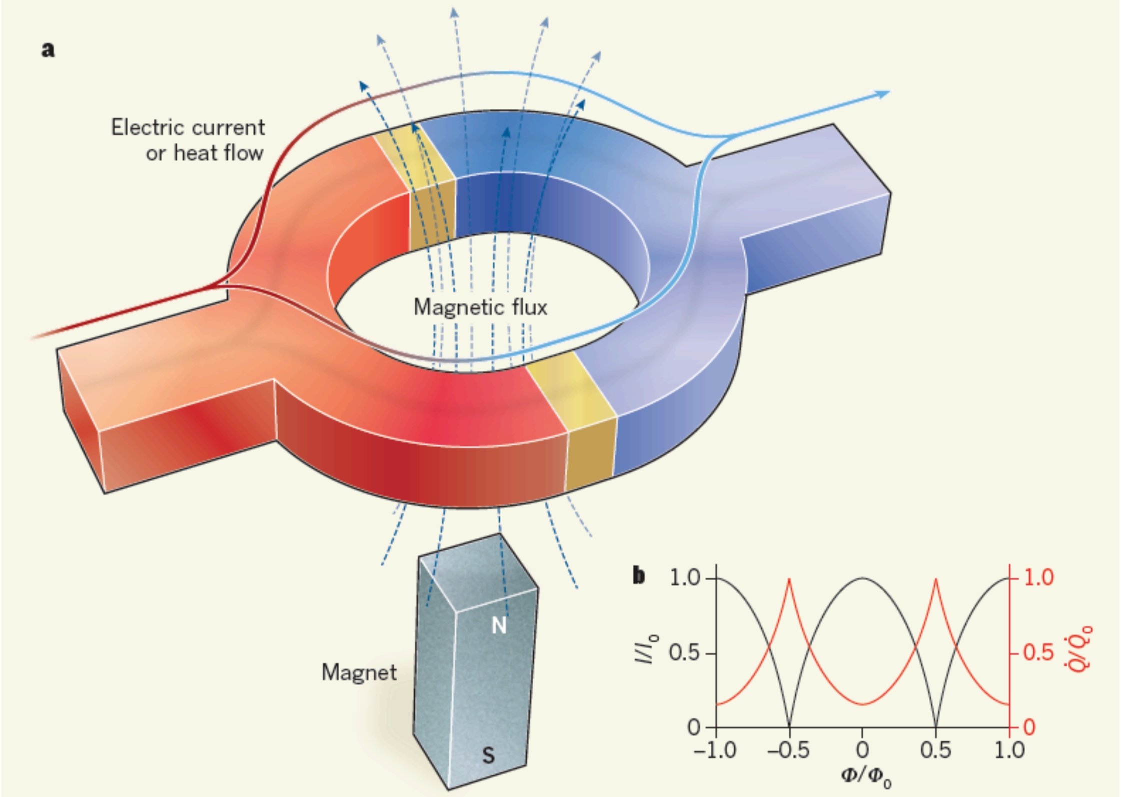

Figure 1 | A direct-current superconducting quantum interference device (d.c.-SQUID). **a**, In d.c.-SQUIDs, a superconducting loop contains two Josephson junctions — thin insulating barriers (yellow) sandwiched between the two superconductors (red and blue). **b**, The maximum electrical current (I, black, left axis) flowing through the device from left to right can be fully modulated by the amount of magnetic flux (Φ) passing through the loop. I_0 is the maximum current that can flow through the d.c.-SQUID; Φ_0 is the magnetic flux quantum, 2.07×10^{-15} webers. Giazotto and Martínez-Pérez[1] have observed an interference effect for heat flow ($\dot{Q}$, red, right axis; $\dot{Q}_0$ is the maximum total heat-flow current) through a d.c.-SQUID: the total amount of heat passing through the device can also be modulated by an applied magnetic flux.

Giazotto and Martinez-Perez
Nature 492, 401 (2012)
News and Views:
R.Simmonds p. 358